

Ergodic Capacity of IRS-Assisted MIMO Systems with Correlation and Practical Phase-Shift Modeling

Anastasios Papazafeiropoulos

Abstract—We focus on the maximization of the exact ergodic capacity (EC) of a point-to-point multiple-input multiple-output (MIMO) system assisted by an intelligent reflecting surface (IRS). In addition, we account for the effects of correlated Rayleigh fading and the intertwinement between the amplitude and the phase shift of the reflecting coefficient of each IRS element, which are usually both neglected despite their presence in practice. Random matrix theory tools allow to derive the probability density function (PDF) of the cascaded channel in closed form, and subsequently, the EC, which depend only on the large-scale statistics and the phase shifts. Notably, we optimize the EC with respect to the phase shifts with low overhead, i.e., once per several coherence intervals instead of the burden of frequent necessary optimization required by expressions being dependent on instantaneous channel information. Monte-Carlo (MC) simulations verify the analytical results and demonstrate the insightful interplay among the key parameters and their impact on the EC.

Index Terms—Intelligent reflecting surface (IRS), ergodic capacity, MIMO communication, correlated Rayleigh fading, beyond 5G networks.

I. INTRODUCTION

Intelligent reflecting surface (IRS) has emerged as a promising green and cost-effective solution towards the sustainable growth of next-generation wireless networks [1]. An IRS is a planar meta-surface, which consists of a large number of nearly passive elements that are managed by a smart controller. The role of each element is the induction of an independent phase shift and/or amplitude attenuation to the impinging electromagnetic waves. In [2], it was shown that the amplitude and phase response are intertwined, while this was neglected by most works. The proper design of the reflecting coefficients enhances the performance by constructive and destructive addition of the signals reflected by IRS to increase the desired signal power and mitigate the co-channel interference, respectively.

The study of IRS performance gains has attracted significant attention under various application scenarios and objectives [3]–[7]. For instance, in [3], a minimization of the total transmit power took place by optimizing the transmit and reflecting beamforming (RB). Also, in [5], we suggested the use of multiple distributed IRSs and compared two practical scenarios, namely, a large number of finite size IRSs and a finite number of large IRSs to show which implementation scenario is more advantageous. Moreover, in [6], we studied the impact of hardware impairments at both the transceiver and IRS sides in a general IRS-assisted multi-user multiple-input single-output (MISO) system with correlated Rayleigh fading, which is usually neglected in relevant works (e.g., see [1], [3]), although it should be taken into account [8]. Furthermore, in [7], the assumptions required to integrate massive multiple-input multiple-output (MIMO) systems with IRS were studied and the achievable rate was obtained.

A. Papazafeiropoulos is with the Communications and Intelligent Systems Research Group, University of Hertfordshire, Hatfield AL10 9AB, U. K., and with the SnT at the University of Luxembourg, Luxembourg. This work was supported by the University of Hertfordshire’s 5-year Vice Chancellor’s Research Fellowship and by the National Research Fund, Luxembourg, under the project RISOTTI. E-mail: tapapazaf@gmail.com

In this direction, most existing works on IRS-assisted systems have focused on single-input single-output (SISO) or MISO systems, while limited research has been devoted to MIMO communication, e.g., see [9]–[11]. In particular, regarding the study of capacity, the capacity limit of point-to-point MIMO IRS-assisted systems was studied in [9] and the capacity region with non-orthogonal multiple access (NOMA) was characterized in [10]. In [11], the ergodic capacity (EC) was studied for SISO channels. Moreover, in [12], the EC for millimeter wave (mmWave) MIMO systems was investigated but not obtained in closed-form. Similarly, in [13], [14], only upper bounds for the EC were derived.

The previous observations motivate the topic of this paper, which is the derivation of the exact EC of MIMO IRS-assisted systems for Rayleigh channels under practical considerations while performing robust optimization. Contrary to [9]–[11], we have accounted for both correlated fading and the intertwinement between the amplitude and phase-shift of each element, which have been disregarded in most previous works. Also, [11] considered only SISO channels, while we focus on MIMO channels. Furthermore, [12] focused on mmWave systems and [13], [14] derived just upper bounds, while these works did not focus on the exact analysis of the EC. To this end, we have achieved to obtain the probability density function (PDF) of an IRS-assisted MIMO channel with correlation in a simple closed-form expression, and we have optimized the EC by considering a practical phase-shift model. Moreover, the optimization in [9], [10] relied on instantaneous channel state information (CSI), while our analytical expression depends only on large-scale statistics as in [5]–[7], and thus, it can be optimized once per several coherence intervals. Hence, our approach is of great value since it achieves to reduce considerably the signal overhead, which becomes prohibitive as the number of IRS elements increases. Finally, we shed light on the impact of the fundamental system parameters on the EC. For example, we show its degradation due to correlated Rayleigh fading.

II. SYSTEM MODEL

We consider a MIMO communication system assisted by a two-dimensional rectangular IRS dynamically adjusted by the IRS controller, where the transmitter and the receiver have M and K , antennas, respectively, as shown in Fig. 1. The IRS, equipped with $N = N_H N_V$ nearly passive reflecting elements, enables the communication between the transmitter and the receiver, where N_H and N_V denote the elements per row and per column of the IRS. Each element has size $d_H d_V$, where d_H is its horizontal width and d_V is the vertical height.

We assume narrowband transmission on quasi-static block-fading channels, where in each block all the channels remain constant. In particular, let $\mathbf{H}_1 = [\mathbf{h}_{1,1}, \dots, \mathbf{h}_{1,M}] \in \mathbb{C}^{N \times M}$ be the channel matrix between the transmitter and the IRS with $\mathbf{h}_{1,i} \in \mathbb{C}^{N \times 1}$ for $i = 1, \dots, M$ being its column vectors. Similarly, $\mathbf{H}_2 \in \mathbb{C}^{K \times N}$ expresses the channel matrix between the IRS and the receiver. The subscripts 1 and 2 correspond to the transmitter-IRS and IRS-receiver links, respectively. Despite that many works, e.g., [3], assumed independent Rayleigh fading model, we take into account the spatial correlations of all nodes, which are unavoidable in practice and affect the

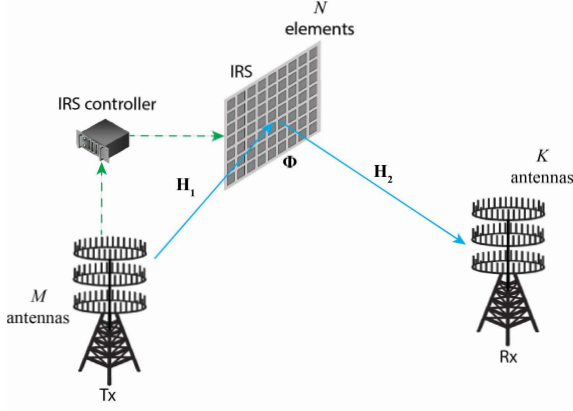


Fig. 1. An IRS-assisted MIMO communication system with M antennas at the transmitter, N IRS elements, and K antennas at the receiver.

performance [8], [15]. Especially, in [8], a correlation model, being suitable for IRS, was presented.

By relying on the Kronecker model to account for the spatial correlation of the MIMO channel for each link, the correlated Rayleigh fading distribution for the i th link can be written as

$$\mathbf{H}_i = \mathbf{R}_i^{\frac{1}{2}} \mathbf{X}_i \mathbf{T}_i^{\frac{1}{2}}, \text{ for } i = 1, 2 \quad (1)$$

where $\mathbf{R}_1 \in \mathbb{C}^{N \times N}$, $\mathbf{T}_1 \in \mathbb{C}^{M \times M}$ and $\mathbf{R}_2 \in \mathbb{C}^{K \times K}$, $\mathbf{T}_2 \in \mathbb{C}^{N \times N}$ describe the deterministic nonnegative semi-definite correlation matrices at the receive, transmit side of link 1 and 2, respectively. Basically, \mathbf{R}_1 and \mathbf{T}_2 , corresponding to the IRS, are identical. Notably, all the correlation matrices, assumed to be known by the network, can be obtained through existing estimation methods (see e.g., [16]). For the IRS, we adopt the suitable correlation model presented in [8], while the correlations at the transmitter and the receiver correspond to conventional linear antenna array modeling (see e.g., [6]). Moreover, $\mathbf{X}_1 \in \mathbb{C}^{N \times M}$ and $\mathbf{X}_2 \in \mathbb{C}^{K \times N}$ express the corresponding fast-fading matrices with elements distributed as $\mathcal{CN}(0, 1)$. Also, β_1 and β_2 denote the path-losses of the transmitter-IRS and IRS-receiver links, respectively.

Let $\Theta = \text{diag}(\alpha_1 e^{j\phi_1}, \dots, \alpha_N e^{j\phi_N}) \in \mathbb{C}^{N \times N}$ denote the reflecting beamforming (RBM) being diagonal and representing the response of the N IRS elements, where $\phi_n \in [-\pi, \pi]$ and $\alpha_n(\phi_n) \in [0, 1]$ express the phase-shift and amplitude coefficient of element n , respectively. Contrary to many previous works that assumed lossless metasurfaces ($\alpha_n(\phi_n) = 1$), we consider that the amplitude coefficient is phase-dependent based on the load or surface impedances as mentioned in [2]. Especially, we consider that the amplitude response is explicitly expressed as a function of the phase shift as

$$\alpha_n(\phi_n) = (1 - \kappa_{\min}) \left(\frac{\sin(\phi_n - \vartheta) + 1}{2} \right)^\xi + \kappa_{\min}, \quad (2)$$

where $\kappa_{\min} \geq 0$ is the minimum amplitude, $\vartheta \geq 0$ is the horizontal distance between $-\pi/2$ and κ_{\min} , which expresses the distance between $-\pi/2$ and the phase shift ϕ_n that minimizes $\sin(\phi_n - \vartheta)$ (i.e., $\phi_n = -\pi/2 + \vartheta$), and ξ is the steepness of the function curve. If $\kappa_{\min} = 1$ or $\xi = 0$, (2) results in the ideal phase-shift model, i.e., $\alpha_n(\phi_n) = 1$.

We assume that signals reflected by the IRS two or more times are ignored and that no direct signal exists due to blockage from obstacles such as buildings. Thus, the effective channel matrix is given by $\mathbf{H}_2 \Theta \mathbf{H}_1$. The received signal vector $\mathbf{y} \in \mathbb{C}^{K \times 1}$ by the receiver is given by

$$\mathbf{y} = \mathbf{H}_2 \Theta \mathbf{H}_1 \mathbf{x} + \mathbf{z}, \quad (3)$$

where \mathbf{x} is the transmit signal vector by the transmitter and $\mathbf{z} \sim \mathcal{CN}(\mathbf{0}, \sigma^2 \mathbf{I}_M)$ is the additive white Gaussian noise (AWGN) vector at the receiver with σ^2 expressing the average noise power.

III. ERGODIC CAPACITY ANALYSIS

By assuming that the transmitter has no channel knowledge while the receiver has perfect CSI of both \mathbf{H}_1 and \mathbf{H}_2 ¹, the EC in (b/s/Hz) of the MIMO-assisted system in (3) is expressed as

$$C = \mathbb{E} \left[\log_2 \det \left(\mathbf{I}_K + \frac{\text{SNR}}{M} \mathbf{H}_2 \Theta \mathbf{H}_1 \mathbf{Q} \mathbf{H}_1^H \Theta^H \mathbf{H}_2^H \right) \right], \quad (4)$$

where the expectation in (4) is over \mathbf{H}_1 , \mathbf{H}_2 while \mathbf{Q} denotes the capacity-achieving input covariance, being normalized by its energy per dimension and given by

$$\mathbf{Q} = \frac{\mathbb{E}[\mathbf{x}\mathbf{x}^H]}{\frac{1}{M} \mathbb{E}[\|\mathbf{x}\|^2]}. \quad (5)$$

Note that the normalization guarantees that $\mathbb{E}[\text{tr}(\mathbf{Q})] = M$. Also, we have

$$\text{SNR} = \frac{\mathbb{E}[\|\mathbf{x}\|^2]}{\frac{1}{K} \sigma^2}. \quad (6)$$

Substitution of the channel expressions described by (1) into (4) gives (7). Next, by denoting $\Lambda_{\mathbf{R}_i}$, $\Lambda_{\mathbf{T}_i}$, and \mathbf{P} the diagonal eigenvalue matrices corresponding to the matrices \mathbf{R}_i , \mathbf{T}_i , and \mathbf{Q} , the EC can be written as in (8). Note that \mathbf{P} describes the capacity-achieving power allocation.

It is generally known that even the derivation of the PDF of the unordered eigenvalue of $\mathbf{H}_i \mathbf{H}_i^H$, where \mathbf{H}_i is given as in (1), is a challenging problem that remains unsolved. In the case of point-to-point MIMO channel, special cases of correlated fading are considered, where correlation is assumed only at either side of the transmitter or the receiver [15]. Also, it is known that doubly correlated Rayleigh fading is not amenable to tractable manipulations [18].

Taking these facts into account, we notice that the capacity expression in (9) includes two random matrices \mathbf{X}_1 , \mathbf{X}_2 while double correlated Rayleigh channels are assumed. To tackle this difficulty, we assume correlation only at the transmitter or the receiver side while we perform singular value decomposition (SVD) to the channel of the other link. Next, we obtain the conditional PDF of the unordered eigenvalue of $\mathbf{G}\mathbf{G}^H$, denoted by $f_{\lambda|\mathbf{L}}$, and finally, we derive the marginal PDF of the unordered eigenvalue. The derivation requires to consider cases, where either $\Lambda_{\mathbf{R}_2} = \mathbf{I}_N$ or $\Lambda_{\mathbf{T}_1} \mathbf{P} = \mathbf{I}_M$ as in [15]. Note that, due to the reciprocity of MIMO channel, correlation at either the receiver or transmitter is equivalent. The only difference is that the former case including $\Lambda_{\mathbf{R}_2}$ is determined completely by the receive correlation while the latter case depends on both the transmit correlation and the power allocation.

A. Main Results

Let us start with $\Lambda_{\mathbf{R}_2} = \mathbf{I}_N$, then after applying the SVD to \mathbf{X}_1 , i.e., $\mathbf{X}_1 = \mathbf{U}_1 \mathbf{D}_1 \mathbf{V}_1^H$, where $\mathbf{D}_1 = \text{diag}(\lambda_1, \dots, \lambda_{\min(M, N)})$ is a diagonal matrix with diagonal elements being the singular values in increasing order while the matrices $\mathbf{U}_1 \in \mathbb{C}^{N \times N}$ and $\mathbf{V}_1 \in \mathbb{C}^{M \times M}$ are unitary and contain the corresponding eigenvectors, we obtain

$$C = \mathbb{E} \left[\log_2 \det \left(\mathbf{I}_K + \frac{\text{SNR}}{M} \mathbf{X}_2 \Psi \mathbf{X}_2^H \right) \right], \quad (9)$$

¹It is worthwhile to mention that by assuming receive RF chains with sensing abilities integrated into the IRS, the acquisition of the CSI of individual channels is feasible as suggested recently in [17]. On this ground, the consideration of the imperfect CSI scenario, which is more practical, is the topic of future work.

$$C = \mathbb{E}[\log_2 \det(\mathbf{I}_K + \frac{\text{SNR}}{M} \mathbf{R}_2 \mathbf{X}_2 \mathbf{T}_2^{\frac{1}{2}} \mathbf{\Theta} \mathbf{R}_1 \mathbf{X}_1 \mathbf{T}_1^{\frac{1}{2}} \mathbf{Q} \mathbf{T}_1^{\frac{1}{2}} \mathbf{X}_1^H \mathbf{R}_1^{\frac{1}{2}} \mathbf{\Theta}^H \mathbf{T}_2^{\frac{1}{2}} \mathbf{X}_2^H)] \quad (7)$$

$$= \mathbb{E}[\log_2 \det(\mathbf{I}_K + \frac{\text{SNR}}{M} \mathbf{\Lambda}_{\mathbf{R}_2} \mathbf{X}_2 \mathbf{\Lambda}_{\mathbf{T}_2}^{\frac{1}{2}} \mathbf{\Theta} \mathbf{\Lambda}_{\mathbf{R}_1}^{\frac{1}{2}} \mathbf{X}_1 \mathbf{\Lambda}_{\mathbf{T}_1} \mathbf{P} \mathbf{X}_1^H \mathbf{\Lambda}_{\mathbf{R}_1}^{\frac{1}{2}} \mathbf{\Theta}^H \mathbf{\Lambda}_{\mathbf{T}_2}^{\frac{1}{2}} \mathbf{X}_2^H)]. \quad (8)$$

where

$$\mathbf{\Psi} = \begin{cases} \text{diag}(\gamma_1(\phi_1)\lambda_1^2, \dots, \gamma_N(\phi_N)\lambda_N^2) & N \leq M \\ \text{diag}(\gamma_1(\phi_1)\lambda_1^2, \dots, \gamma_M(\phi_M)\lambda_M^2, \underbrace{0, \dots, 0}_{N-M}) & N > M \end{cases} \quad (10)$$

with $\gamma_i(\phi_i) = p_i \alpha_i^2(\phi_i) \lambda_{\mathbf{T}_1, i} \lambda_{\mathbf{R}_1, i} \lambda_{\mathbf{T}_2, i}$. Note that we have taken into account the invariance of \mathbf{X}_2 under left and right unitary transformation and that to achieve capacity (optimal transmit strategy), the eigenvectors of \mathbf{Q} must coincide with those of the transmit correlation \mathbf{T}_1 [15]. Since the transmitter has no channel knowledge, equal power allocation to each transmit antenna is the most reasonable strategy, i.e., choosing $\mathbf{Q} = \frac{P}{M} \mathbf{I}_M$ (see [18] and references therein). Hence, the required EC optimization below concerns only the phase shifts. More concretely, we can write

$$C = \mathbb{E}[\log_2 \det(\mathbf{I}_K + \frac{\text{SNR}}{M} \hat{\mathbf{X}}_2 \hat{\mathbf{L}} \hat{\mathbf{X}}_2^H)], \quad (11)$$

where $\hat{\mathbf{X}}_2 \sim \mathcal{CN}(\mathbf{0}, \mathbf{I}_K \otimes \mathbf{I}_q)$ and $\hat{\mathbf{L}} = \text{diag}(\gamma_i(\phi_i)\lambda_i^2)_{i=1}^q$ with $q = \min(M, N)$.

Similarly, if we set $\mathbf{\Lambda}_{\mathbf{T}_1} \mathbf{P} = \mathbf{I}_M$ and apply the SVD to \mathbf{X}_2 , which means $\mathbf{X}_2 = \mathbf{U}_2 \mathbf{D}_2 \mathbf{V}_2^H$, where $\mathbf{D}_2 = \text{diag}(\tilde{\lambda}_1, \dots, \tilde{\lambda}_{\min(K, N)})$ is a diagonal matrix with diagonal elements being the singular values in increasing order while $\mathbf{U}_2 \in \mathbb{C}^{K \times K}$ and $\mathbf{V}_2 \in \mathbb{C}^{N \times N}$ are unitary matrices, we obtain

$$C = \mathbb{E}[\log_2 \det(\mathbf{I}_M + \frac{\text{SNR}}{M} \mathbf{X}_1^H \tilde{\mathbf{\Psi}} \mathbf{X}_1)], \quad (12)$$

where

$$\tilde{\mathbf{\Psi}} = \begin{cases} \text{diag}(\tilde{\gamma}_1(\phi_1)\tilde{\lambda}_1^2, \dots, \tilde{\gamma}_N(\phi_N)\tilde{\lambda}_N^2) & N \leq K \\ \text{diag}(\tilde{\gamma}_1(\phi_1)\tilde{\lambda}_1^2, \dots, \tilde{\gamma}_K(\phi_K)\tilde{\lambda}_K^2, \underbrace{0, \dots, 0}_{N-K}) & N > K \end{cases} \quad (13)$$

with $\tilde{\gamma}_i(\phi_i) = p_i \alpha_i^2(\phi_i) \lambda_{\mathbf{R}_1, i} \lambda_{\mathbf{R}_2, i} \lambda_{\mathbf{T}_2, i}$ and the invariance of \mathbf{X}_1 considered under left and right unitary transformation. In a similar way to (11), the capacity can be described by

$$C = \mathbb{E}[\log_2 \det(\mathbf{I}_M + \frac{\text{SNR}}{M} \tilde{\mathbf{X}}_1^H \tilde{\mathbf{L}} \tilde{\mathbf{X}}_1)], \quad (14)$$

where $\tilde{\mathbf{X}}_1 \sim \mathcal{CN}(\mathbf{0}, \mathbf{I}_M \otimes \mathbf{I}_{\tilde{q}})$ and $\tilde{\mathbf{L}} = \text{diag}(\tilde{\gamma}_i(\phi_i)\tilde{\lambda}_i^2)_{i=1}^{\tilde{q}}$ with $\tilde{q} = \min(K, N)$.

We observe that (11) and (14) have a similar expression. Hence, it is sufficient to compute one of them, e.g., (11). We can rewrite it in an equivalent way as

$$\hat{C} = s \int_0^\infty \log_2 \left(1 + \frac{\text{SNR}}{M} \hat{\lambda} \right) f_{\hat{\lambda}}(\hat{\lambda}) d\hat{\lambda}, \quad (15)$$

where $s = \min(K, q)$, $\hat{\lambda}$ is an unordered eigenvalue of the random matrix $\hat{\mathbf{X}}_2 \hat{\mathbf{L}} \hat{\mathbf{X}}_2^H$, and $f_{\hat{\lambda}}(\hat{\lambda})$ is its PDF. Notably, there is no expression for the distribution of $\hat{\lambda}$. We notice that (15) resembles [18, Eq. 11] but includes a different form of the diagonal matrix, which can not result in our expressions as a special case. Remarkably, (15) provides the EC an IRS-assisted MIMO channel with correlation in terms of large-scale statistics.

For this reason, it is required first to obtain a new exact closed-form expression for the joint PDF of $0 \leq c_1 < \dots < c_q < \infty$, where $c_i = \gamma_i(\phi_i)\lambda_i^2$ are the elements of $\hat{\mathbf{L}}$.

Lemma 1: The joint pdf of $\hat{\mathbf{L}} = \text{diag}(c_1, \dots, c_q)$, where $0 \leq c_1 < \dots < c_q < \infty$, is given by

$$f_{\hat{\mathbf{L}}}(c_1, \dots, c_q) = \mathcal{K} \prod_{i=1}^q \frac{c_i^{p-q} e^{-\frac{c_i}{\gamma_i}}}{\gamma_i^{p-q+1}} \prod_{i < j}^q \left(\frac{c_j}{\gamma_j} - \frac{c_i}{\gamma_i} \right)^2, \quad (16)$$

where $\mathcal{K} = (\prod_{i=1}^q \Gamma(q-i+1) \Gamma(p-i+1))^{-1}$ with $p = \max(K, N)$.

Proof: See Appendix A. ■

Taking into account Lemma 1, we obtain $f_{\hat{\lambda}}(\hat{\lambda})$ according to the following theorem.

Theorem 1: The marginal PDF of an unordered eigenvalue $\hat{\lambda}$ of $\mathbf{X}_1^H \tilde{\mathbf{L}} \mathbf{X}_1$ is given by

$$f_{\hat{\lambda}}(\hat{\lambda}) = \frac{\mathcal{K}}{s \prod_{i < j}^q (\gamma_j - \gamma_i)} \sum_{l=1}^q \sum_{k=q-s+1}^q \frac{\hat{\lambda}^{(M+p-2q+2k+l-3)/2}}{\Gamma(M-q+k) \gamma_l^{\frac{p-M+l-1}{2}}} \times K_{p-M+l-1}(2\sqrt{\hat{\lambda}/\gamma_l}) G_{l,k}, \quad (17)$$

where $G_{l,k}$ is the (l, k) th cofactor of a $q \times q$ matrix whose (m, n) th entry is $\{\mathbf{G}\}_{m,n} = \Gamma(p-q+m+n-1)$.

Proof: See Appendix B. ■

Remark 1: Theorem 1 presents the PDF of an IRS-assisted MIMO channel with correlation in a simple closed-form expression. Based on this theorem, the EC in (15) depends on the number of antennas at the transmitter, the receiver, and the number or IRS elements together with the eigenvalues of the correlation matrices. A notable dependence in (17) concerns the phase-shift and amplitude in terms of $\alpha_i^2(\phi_i)$.

B. RBM optimization

The EC can be maximized in terms of the phase shifts. Relying on the common assumption of infinite resolution phase shifters, we formulate the optimization problem as

$$(\mathcal{P}1) \quad \max_{\Phi} \hat{C} \\ \text{s.t.} \quad -\pi \leq \phi_n \leq \pi, \quad n=1, \dots, q, \quad (18)$$

where \hat{C} is given by (15) based on (11) or (14).

The problem ($\mathcal{P}1$) concerns a non-convex maximization with respect to ϕ_n . Taking the expression of $f_{\hat{\lambda}}(\hat{\lambda})$ into account, the optimization of (15) is basically a constrained maximization problem whose solution could be given by means of the projected gradient ascent until convergence to a stationary point [6]. The convergence is guaranteed due to the power constraint. Since the dependence on phase shifts is hidden only in $f_{\hat{\lambda}}(\hat{\lambda})$, below, we focus on their optimization. According to the algorithm, let $\mathbf{s}^i = [\phi_1^i, \dots, \phi_q^i]^T$ denote the vector including the phases at step i . The next iteration point results in the increase of $f_{\hat{\lambda}}(\hat{\lambda})$ towards to its convergence. Hence, we have

$$\tilde{\mathbf{s}}^{i+1} = \mathbf{s}^i + \mu \mathbf{q}^i, \quad (19)$$

$$\mathbf{s}^{i+1} = \exp(j \arg(\tilde{\mathbf{s}}^{i+1})), \quad (20)$$

where μ is the step size and \mathbf{q}^i is the adopted ascent direction at step i with $[\mathbf{q}^i]_n = \frac{\partial f_{\hat{\lambda}}(\hat{\lambda})}{\partial \phi_n}$. This derivative is provided by Lemma 2 below. The solution is found by formulating the projection problem $\min_{|\phi_n|=1, n=1, \dots, N} \|\mathbf{s} - \tilde{\mathbf{s}}\|^2$ based on (19) and (20) under the constraint in (18). Note that the suitable step size requires computation at each iteration, which is achieved by means of the backtracking line search [19].

Lemma 2: The derivative of $f_{\hat{\lambda}}(\hat{\lambda})$ with respect to ϕ_n is provided by

$$\begin{aligned} \frac{\partial f_{\hat{\lambda}}(\hat{\lambda})}{\partial \phi_n} = & -\frac{p_n \alpha_n(\phi_n) \lambda_{\mathbf{T}_1, n} \lambda_{\mathbf{R}_1, n} \lambda_{\mathbf{T}_2, n} \mathcal{K}}{s \prod_{i < j}^q (\gamma_j - \gamma_i)} (1 - \kappa_{\min}) \xi \\ & \times \cos(\phi_n - \vartheta) \left(\frac{\sin(\phi_n - \vartheta) + 1}{2} \right)^{\xi-1} (\text{tr}(\mathbf{V}^{-1} \frac{\partial \mathbf{V}}{\partial \gamma_n})) \\ & \times \sum_{l=1}^q \sum_{k=q-s+1}^q \frac{\hat{\lambda}^{(M+p-2q+2k+l-3)/2}}{\Gamma(M-q+k) \gamma_l^{\frac{p-M+l-1}{2}}} \mathbf{K}_{p-M+l-1}(2\sqrt{\hat{\lambda}/\gamma_l}) G_{l,k} \\ & + \sum_{k=q-s+1}^q \frac{\hat{\lambda}^{(2M+\bar{p}-2q+2k-2)/2}}{\Gamma(M-q+k) \gamma_n^{\frac{\bar{p}}{2}}} G_{n,k} \left(\frac{\bar{p}}{2\gamma_n} \mathbf{K}_{\bar{p}}(2\sqrt{\hat{\lambda}/\gamma_n}) \right. \\ & \left. - \frac{1}{\gamma_n} \sqrt{\frac{\hat{\lambda}}{\gamma_n}} (\mathbf{K}_{\bar{p}-1}(2\sqrt{\hat{\lambda}/\gamma_n}) + \mathbf{K}_{\bar{p}+1}(2\sqrt{\hat{\lambda}/\gamma_n})) \right), \quad (21) \end{aligned}$$

where $\bar{p} = p - M + n - 1$, \mathbf{V} is the Vandermonde matrix satisfying $\det(\mathbf{V}) = \prod_{i < j}^q (\gamma_j - \gamma_i)$, and $\frac{\partial \mathbf{V}}{\partial \gamma_n}$ is a matrix whose elements are the derivatives of \mathbf{V} with respect to γ_n .

Proof: The computation of the derivative is straightforward since $f_{\hat{\lambda}}(\hat{\lambda})$ is in closed-form. We notice that the dependence on the phase shifts is inside γ_l in terms of $\alpha_l^2(\phi_l)$. Hence, the derivative is obtained as in (21) by using the derivative of (2), [20, Eq. 46], which gives the derivative of a determinant, and [21, Eq. 03.04.20.0014.02], which gives the derivative of $K_v(\cdot)$ after some simple algebraic manipulations. ■

IV. NUMERICAL RESULTS

We consider uniform linear arrays (ULAs) for the configuration of both the transmitter and the receiver, while the IRS consists of a uniform planar array (UPA). Based on the 3GPP Urban Micro (UMi) scenario from TR36.814 for a carrier frequency of 2.5 GHz and noise level -80 dBm, the path losses for \mathbf{H}_1 and \mathbf{H}_2 are generated based on the NLOS version [22]. Specifically, therein, the overall path loss for the IRS-assisted link is $\beta = \beta_1 \beta_2$, where $\beta_i = C_i d_i^{-\nu_i}$, $i = 1, 2$ with $C_1 = 26$ dB, $C_2 = 28$ dB, $\nu_1 = 2.2$, $\nu_2 = 3.67$. The variables $d_1 = 8$ m and $d_2 = 60$ m express the distances between the transmitter and the IRS, and the IRS and the receiver, respectively. As can be seen, since the IRS is closer to the transmitter, the path-loss exponent of this link is lower because fewer obstacles are expected. We use 5 dBi antennas at the transmitter ($M = 4$) and the receiver ($K = 4$), and their correlation matrices are given by [6]. Unless otherwise stated, we consider the following values. The correlation matrix for the IRS is given by [8], where $d_H = d_V = \lambda/4$. The phase shift model parameters are $\kappa_{\min} = 0.8$, $\xi = 1.6$, and $\vartheta = 0.43\pi$ [2]. The figures correspond to $\mathbf{\Lambda}_{\mathbf{R}_2} = \mathbf{I}_N$, while similar observations can be extracted in the case $\mathbf{\Lambda}_{\mathbf{T}_1} \mathbf{P} = \mathbf{I}_M$ since we do not focus on the transceiver design but on the impact of the IRS. Furthermore, Monte-Carlo (MC) simulations coincide with the analytical results in all cases, which corroborates our analysis.

Fig. 2 illustrates the EC versus the number of IRS elements. In general, we observe that \hat{C} increases with the number of IRS elements. Moreover, given specific values for the phase-shift model, we study the impact of the IRS correlation. We observe that the unrealistic independent Rayleigh fading gives

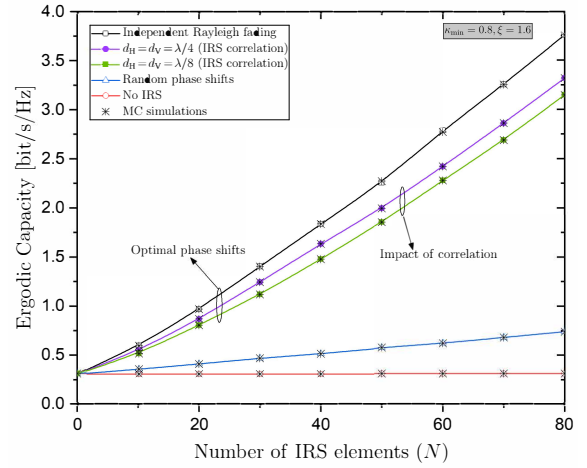


Fig. 2. EC of an IRS-assisted MIMO system versus the number of IRS elements N for varying IRS correlation ($\kappa_{\min} = 0.8$, $\xi = 1.6$).

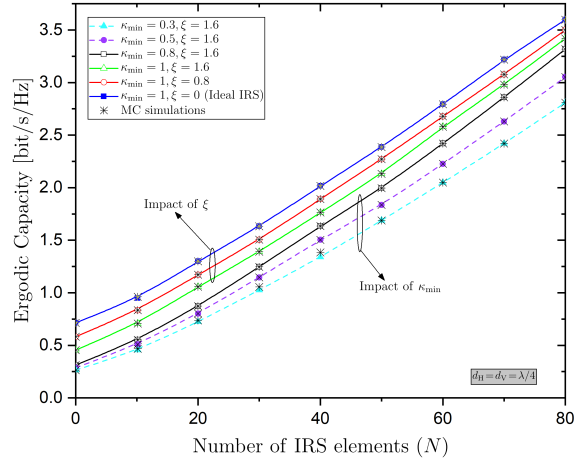


Fig. 3. EC of an IRS-assisted MIMO system versus the number of IRS elements N for varying phase-shift model parameters ($d_H = d_V = \lambda/8$).

the highest \hat{C} , while the decrease of the distance between the IRS elements (higher correlation) results in a lower capacity. Also, we depict the scenarios with no IRS and with random phase shifts, i.e., not optimized. The former corresponds to a horizontal line as N increases since the capacity is independent of N , while the latter shows that the phase-shift optimization is clearly very beneficial during the IRS implementation.

In Fig. 3, we depict the EC for different phase-shift settings. The “dashed” and “solid” lines correspond to variation of κ_{\min} and ξ , respectively. For the sake of comparison, we have also shown the case of ideal phase-shift model ($\kappa_{\min} = 1$, $\xi = 0$). We observe that when κ_{\min} increases, EC increases. On the contrary, when ξ increases, \hat{C} decreases. Notable, these observations coincide with the results in [11] for SISO-IRS assisted channels.

V. CONCLUSION

In this paper, we derived the PDF and the EC of a point-to-point MIMO system assisted by an IRS under the unavoidable realistic conditions of correlated Rayleigh fading and correlation between the amplitude and the phase-shift of each IRS element. Also, we provided the maximization of the EC with respect to the phase shifts of the IRS elements. This maximization is advantageous since it is accompanied by

reduced overhead and computational complexity by exploiting the dependence of the EC by just large-scale statistics. The analytical results are verified by MC simulations and show how the various system parameters affect the EC. For example, correlated fading results in performance degradation. Future works on EC should account for Rician fading conditions, and possibly, the existence of a direct path between the transmitter and the receiver.

APPENDIX A PROOF OF LEMMA 1

The joint PDF of $\mathbf{W} = \text{diag}(w_1, \dots, w_q)$, where $w_i = \hat{\lambda}_i^2$ and $p = \max(K, N)$, is given by [23] as

$$f_{\mathbf{W}}(w_1, \dots, w_q) = \mathcal{K} e^{-\sum_{i=1}^q w_i} \prod_{i=1}^q w_i^{p-q} \prod_{i < j} (w_j - w_i)^2. \quad (22)$$

Taking into account that $\hat{\lambda}_i^2 = c_i/\gamma_i(\phi_i)$, we obtain the joint PDF of $\hat{\mathbf{L}} = \text{diag}(c_1, \dots, c_q)$ after applying a vector transformation to (22) as

$$f_{\hat{\mathbf{L}}}(c_1, \dots, c_q) = f_{\mathbf{W}}\left(\frac{c_1}{\gamma_1}, \dots, \frac{c_q}{\gamma_q}\right) \times |\mathbf{J}((w_1, \dots, w_q) \rightarrow (c_1, \dots, c_q))|, \quad (23)$$

where the Jacobian transformation is evaluated as

$$|\mathbf{J}((w_1, \dots, w_q) \rightarrow (c_1, \dots, c_q))| = \prod_{i=1}^q \frac{1}{\gamma_i}. \quad (24)$$

Substitution of (22) and (24) into (23) gives the joint PDF of $\hat{\mathbf{L}}$ in (16).

APPENDIX B PROOF OF THEOREM 1

The unconditional PDF of an unordered eigenvalue of $\mathbf{X}_1^H \hat{\mathbf{L}} \mathbf{X}_1$ is obtained by taking the expectation over $\hat{\mathbf{L}}$, i.e., $\mathbb{E}_{\hat{\mathbf{L}}}[f_{\hat{\lambda}|\hat{\mathbf{L}}}(\hat{\lambda})]$. For this reason, we employ the conditional unordered eigenvalue PDF from [18, Lemma 1] after expressing it as

$$f_{\hat{\lambda}|\hat{\mathbf{L}}}(\hat{\lambda}) = \frac{1}{s \prod_{i < j}^q (c_j - c_i)} \sum_{k=q-s+1}^q \frac{\hat{\lambda}^{M-q+k-1}}{\Gamma(M-q+k)} \det(\mathbf{D}_k), \quad (25)$$

where \mathbf{D}_k is a $q \times q$ matrix with entries

$$\{\mathbf{D}_k\}_{m,n} = \begin{cases} c_m^{n-1}, & n \neq k, \\ e^{-\hat{\lambda}/c_m} c_m^{q-M-1}, & n = k. \end{cases} \quad (26)$$

The unconditional PDF is derived as

$$f_{\hat{\lambda}}(\hat{\lambda}) = \frac{\mathcal{K}}{s} \sum_{k=q-s+1}^q \frac{\hat{\lambda}^{M-q+k-1}}{\Gamma(M-q+k)} \mathcal{I}_k, \quad (27)$$

where

$$\mathcal{I}_k = \int_{0 \leq c_1 < \dots < c_q < \infty} \det(\mathbf{D}_k) \prod_{i=1}^q c_i^{p-q} e^{-\frac{c_i}{\gamma_i}} \prod_{i < j}^q \frac{\left(\frac{c_j}{\gamma_j} - \frac{c_i}{\gamma_i}\right)^2}{(c_j - c_i)} dc_1 \dots dc_q.$$

Meanwhile, according to the matrix theory, it holds that $\prod_{i < j}^q (\theta_j - \theta_i) = \det(\mathbf{X})$, where \mathbf{X} is a Vandermonde matrix with entry given by θ_i^{j-1} . Based on this property, we obtain

$$\mathcal{I}_k = \frac{1}{\prod_{i < j}^q (\gamma_j - \gamma_i)} \det(\mathbf{Y}_k), \quad (28)$$

where \mathbf{Y}_k is a $q \times q$ matrix with entries

$$\{\mathbf{Y}_k\}_{m,n} = \begin{cases} \int_0^\infty x^{p-q+m+n-2} e^{-x} dx, & n \neq k, \\ \int_0^\infty e^{-\hat{\lambda}/\gamma_l x} x^{p-M+m-2} e^{-x} dx, & n = k. \end{cases} \quad (29)$$

Note that in (29), we have made a change of variables, i.e., we have set $x = c_l/\gamma_l$. The integrals are evaluated based on [24, Eq.3.381.4] and [24, Eq.3.471.9] as

$$\int_0^\infty x^{p-q+m+n-2} e^{-x} dx = \Gamma(p-q+m+n-1), \quad (30)$$

$$\int_0^\infty e^{-\hat{\lambda}/\gamma_l x} x^{\tilde{p}-1} e^{-x} dx = 2 \left(\frac{\hat{\lambda}}{\gamma_l}\right)^{\frac{\tilde{p}}{2}} K_{\tilde{p}}(2\sqrt{\hat{\lambda}/\gamma_l}), \quad (31)$$

where $\tilde{p} = p - M + m - 1$, $K_\nu(\cdot)$ is the modified Bessel function of the second kind [24, Eq. 8.432.6]. Substitution of (30) and (31) into (29) together with the application of Laplace's expansion provides the desired result.

REFERENCES

- [1] E. Basar *et al.*, "Wireless communications through reconfigurable intelligent surfaces," *IEEE Access*, vol. 7, pp. 116 753–116 773, 2019.
- [2] S. Abeywickrama *et al.*, "Intelligent reflecting surface: Practical phase shift model and beamforming optimization," *IEEE Trans. Commun.*, vol. 68, no. 9, pp. 5849–5863, 2020.
- [3] Q. Wu and R. Zhang, "Intelligent reflecting surface enhanced wireless network via joint active and passive beamforming," *IEEE Trans. Wireless Commun.*, vol. 18, no. 11, pp. 5394–5409, 2019.
- [4] A. M. Elbir *et al.*, "Deep channel learning for large intelligent surfaces aided mm-Wave massive MIMO systems," *IEEE Wireless Commun. Lett.*, vol. 9, no. 9, pp. 1447–1451, 2020.
- [5] A. Papazafeiropoulos *et al.*, "Coverage probability of distributed IRS systems under spatially correlated channels," vol. 10, no. 8, pp. 1722–1726, 2021.
- [6] A. Papazafeiropoulos *et al.*, "Intelligent reflecting surface-assisted MU-MISO systems with imperfect hardware: Channel estimation, beamforming design," *IEEE Trans. Wireless Commun.*, 2021.
- [7] Z. Wang *et al.*, "Massive MIMO communication with intelligent reflecting surface," *arXiv preprint arXiv:2107.04255*, 2021.
- [8] E. Björnson and L. Sanguinetti, "Rayleigh fading modeling and channel hardening for reconfigurable intelligent surfaces," *IEEE Wireless Commun. Lett.*, vol. 10, no. 4, pp. 830–834, 2021.
- [9] S. Zhang and R. Zhang, "Capacity characterization for intelligent reflecting surface aided MIMO communication," *IEEE J. Sel. Areas Commun.*, vol. 38, no. 8, pp. 1823–1838.
- [10] X. Mu *et al.*, "Capacity and optimal resource allocation for IRS-assisted multi-user communication systems," *IEEE Trans. Commun.*, vol. 69, no. 6, pp. 3771–3786, 2021.
- [11] Y. Zhang *et al.*, "Performance analysis of RIS-aided systems with practical phase shift and amplitude response," *IEEE Trans. Veh. Tech.*, vol. 70, no. 5, pp. 4501–4511, 2021.
- [12] C. Guo *et al.*, "Maximum ergodic capacity of intelligent reflecting surface assisted MIMO wireless communication system," in *International Conference on Communications and Networking in China*. Springer, 2019, pp. 331–343.
- [13] F. Yang *et al.*, "Intelligent reflecting surface-assisted mmWave communication exploiting statistical CSI," in *IEEE International Conference on Communications (ICC)*, 2020, pp. 1–6.
- [14] J. Wang *et al.*, "Joint transmit beamforming and phase shift design for reconfigurable intelligent surface assisted MIMO systems," *IEEE Trans. Cogn. Commun. Net.*, vol. 7, no. 2, pp. 354–368, 2021.
- [15] G. Alfano *et al.*, "Capacity of MIMO channels with one-sided correlation," in *Eighth IEEE International Symposium on Spread Spectrum Techniques and Applications-Programme and Book of Abstracts*, pp. 515–519.
- [16] D. Neumann, M. Joham, and W. Utschick, "Covariance matrix estimation in massive MIMO," *IEEE Signal Process. Lett.*, vol. 25, no. 6, pp. 863–867, 2018.
- [17] B. Zheng, C. You, and R. Zhang, "Efficient channel estimation for double-IRS aided multi-user MIMO system," vol. 69, no. 6, pp. 3818–3832.
- [18] S. Jin *et al.*, "Ergodic capacity analysis of amplify-and-forward MIMO dual-hop systems," *IEEE Trans. on Inform. Theory*, vol. 56, no. 5, pp. 2204–2224, 2010.
- [19] S. Boyd, S. P. Boyd, and L. Vandenberghe, *Convex optimization*. Cambridge university press, 2004.
- [20] K. B. Petersen and M. S. Pedersen, "The matrix cookbook, nov 2012," URL <http://www2.imm.dtu.dk/pubdb/p.php>, vol. 3274, p. 14, 2012.
- [21] T. W. f. s. Wolfram. [Online]. Available: <http://functions.wolfram.com>
- [22] 3GPP, "Further advancements for E-UTRA physical layer aspects (Release 9)," 3GPP TS 36.814, Tech. Rep., 2017.
- [23] A. T. James, "Distributions of matrix variates and latent roots derived from normal samples," *The Ann. of Math. Statist.*, pp. 475–501, 1964.
- [24] I. S. Gradshteyn and I. M. Ryzhik, "Table of integrals, series, and products," *Alan Jeffrey and Daniel Zwillinger (eds.), Seventh edition (Feb 2007)*, vol. 885, 2007.